Joint Estimation for Battery Capacity and the State of Charge Based on Variable Time Scale

Yu, Man

School of Vehicle Engineering, Xi'an Aeronautical Institute, Xi'an, P.R. CHINA

Yu, Qiang*+; Li, Meiying

Transportation Industry Key Laboratory of Automobile Transportation Safety Assurance Technology, Chang'an University, Xi'an, P.R. CHINA

ABSTRACT: *As the core energy source of electric vehicles, power batteries directly restrict the development of electric vehicles. Accurate estimation of SOC is not only the fundamental function of the electric vehicle battery management system but also helps to improve energy utilization of batteries, safeguard the application of batteries in EVs, and extend the cycling life. However, the time-varying nonlinearity, environmental sensitivity, and irreversible decay during the use of the battery make the estimation of hidden states such as SOC a challenge to the industry. This study conducted the following research on the SOC and capacity estimation of lithium-ion batteries: (1) To achieve the co-estimation of the battery's state and parameters, an adaptive cubature Kalman filter SOC estimation method based on random weighting (ARWCKF) is proposed, at the same time, Extended Kalman Filter (EKF) is used to identify the parameter on-line. The results verify that this approach has a better performance with the error of SOC being under 3%. (2) Aiming at the limitations of the single-time-scale joint estimation algorithm, taking accumulated discharge as the conversion standard between micro and macro time scales. The filtering performance of the algorithm is effectively evaluated based on the prediction accuracy of the terminal voltage, SOC, capacity, and the convergence rate of SOC and capacity, verifying that compared to the single-time-scale approach, this approach has better robustness and accuracy.*

KEYWORDS: *Vehicle engineering; Lithium-ion battery; Cubature Kalman filter; State of charge; Capacity; co-estimation.*

INTRODUCTION

SOC is usually used to measure the remaining available capacity of power batteries quantitatively and is one of the most important parameters of electric vehicles. Related studies show that the electrochemical reaction process, impedance parameters, and external characteristic parameters of power battery vary greatly in different SOC, so it is necessary to determine the value of SOC when analyzing the internal and external characteristic parameters of power battery [1-3]. Furthermore, a series of battery management strategies, such as battery charge-discharge

** To whom correspondence should be addressed.*
+ E-mail: *qiangyu@chd.edu.cn & zhao.72@bk.ru*
1021-9986/2021/6/1943-1959 17/$/6.07

control, health state estimation, and fault diagnosis are inseparable from accurate SOC estimation. Constituting a reasonable battery management strategy is helpful to prolong battery life, preventing battery over-discharge and improving battery safety factors [4,5]. Accurate SOC estimation also contributes to the optimization of vehicle energy management strategy, to the greatest extent improving energy efficiency and increasing driving mileage as much as possible [6]. But at the same time, due to the complexity and variability of the battery's internal structure and electrochemical reaction, and the uncertainty of the actual operating conditions, it is difficult to accurately estimate stealth state quantities of SOC in real-time [7-9]. In addition, battery capacity as an important indicator to measure battery aging and health status is as important and closely related as SOC. But the battery capacity is not a fixed value, which is closely related to the using conditions and aging status of the power battery.

The co-estimation of SOC and capacity is based on the external charge-discharge characteristics of the power battery. At the same time, using the relationship between SOC and capacity, the mutual correction between SOC and capacity is realized based on the same error feedback information, so as to improve the prediction accuracy of SOC and capacity. *Gregory L Plett et al.* realized the co-estimation of SOC and capacity based on the double extend Kalman filter (EKF) algorithm for the first time and formed a closed-loop feedback structure between capacity estimation and SOC estimation, which laid the groundwork for subsequent joint battery state estimation research [10]. *Lee* analyzed the relationship between battery aging and OCV-SOC curve in detail, and improved the OCV-SOC curve, so as to solve the failure problem of the double EKF algorithm to estimate available capacity caused by battery aging [11]. However, due to the complexity and variability of the battery's internal structure and electrochemical reaction, and the uncertainty of the actual operating conditions, it is difficult to accurately estimate stealth state quantities of SOC and capacity in real-time [7-9].

In recent years, filtering methods were improved constantly in the state estimation area, and a large number of scholars have fused equivalent circuit models with Kalman Filter to update battery states. Such as the Cubature Kalman Filter (CKF), which is commonly used in the field of the non-linear filter. Compared with the unscented Kalman Filter (UKF), it uses the third-order spherical-radial volume criterion to approximate the probability density function, and the weights of the sampling points are the same and are positive, so its numerical value stability and filtering accuracy are higher than UKF [12,13]. The reference [14] proposed square root cubature Kalman filter (SCKF), which iterates the square root of the error covariance matrix, so ensures the symmetry and non-negative definiteness of the covariance matrix, and finally improves the filtering accuracy of the system. However, CKF also requires accurate priori statistical information of known measurement noise, and the filtering accuracy will decrease or even diverge when there is uncertainty in the statistical characteristics of measurement noise. In order to solve this problem, the reference [15-17] improves the CKF based on the moving windowing method to obtain an adaptive ASCKF algorithm, which estimates and adjusts the statistical characteristics of the measurement noise in real-time with the help of the moving windowing technique. However, because the ASCKF algorithm takes the same weight 1/n to the information at different times in the window and ignores the difference in the contribution of the information at different times, it can't accurately estimate the statistical characteristics of the measurement noise, which has a certain impact on the filtering accuracy. In addition, with the development of various algorithm technologies, data-based machine learning methods have been increasingly applied to SOC estimation. *Mahmood et al.* reviewed the basics of machine learning and common procedures for applying machine learning [18-19], which provide a theoretical basis and option for SOC estimation algorithms. While the method of machine learning relies heavily on model data, how to meet a large number of data requirements in actual operation is a difficult problem that needs to be solved.

This dissertation takes the power battery management system of an electric vehicle as the research object and carries out related research on the state estimation of power batteries at different times. The 1-order RC model with high model accuracy and moderate model complexity is selected as the model basis, and then the improved cubature Kalman filter algorithm is used to realize the real-time SOC estimation. In view of the influence of capacity on SOC estimation, a more robust co-estimation method of variable-time-scale SOC and capacity is proposed. The accuracy and timeliness of the proposed method are verified, which is of great significance

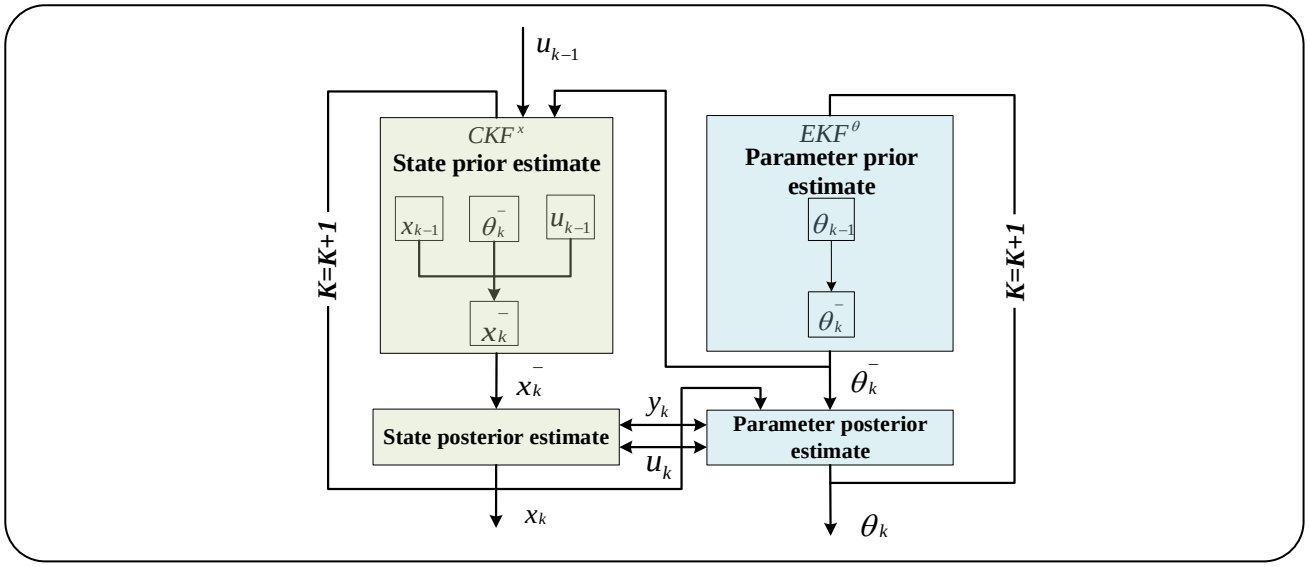

Fig. 1: Algorithm Schematic of EKF-CKF Filter.

to ensure the stability and safety of electric vehicles during the actual operation process.

EXPERIMENTAL SECTION

The proposal for EKF—CKF filtering

Considering that there is no effective feedback correction between parameter identification and state estimation in the traditional Kalman filtering process based on online parameter identification, this dissertation proposes the EKF-CKF filtering theory, therefore, in this dissertation, the EKF filter is used for the online identification of the model parameters, and the CKF filter is used for the real-time state estimation of the system. The process of parameter identification and state estimation is modified by the same observation equation respectively, which realizes the co-convergence process of the state and parameters, and improves the stability of the algorithm. Next, the EKF-CKF algorithm is described in detail.

Establish a non-linear discrete system as follows:

$$\begin{cases} x_k = f(x_{k-1}, \theta_{k-1}, u_{k-1}) + w_{k-1} \\ \theta_k = \theta_{k-1} + \rho_{k-1} \\ y_k = g(x_k, \theta_k, u_k) + v_k \end{cases} \quad (1)$$

Where, $f(x_k,u_k)$ and $g(x_k,u_k)$ respectively represent the state transfer function and observation function of a non-linear system; x_k represents the state vector at k-moment, y_k represents the observation at k-moment; θ_k represents the parameter matrix at k-moment; process the noise of the parameter equation at k-moment is ρ_k, and its statistical characteristics are unknown and unlimited. In this dissertation, the upper right corner is unified and used to distinguish between the state estimation process and the parameter identification process, that is to say, P_k^x represents the state estimation process and P_k^θ represents the parameter identification process.

After completing the above basic work, the principle of the EKF-CKF filtering algorithm established in this dissertation is shown in Fig 1, and the concrete algorithm steps are as follows.

Algorithm initialization: parameter initialization of parameter observer EKF$^\theta$ and state observer CKF^x

$$\theta_0, P_0^\theta, Q_0^\theta, R_0^\theta, x_0, P_0^x, Q_0^x, R_0^x \quad (2)$$

In which, $\theta_0, P_0^\theta, Q_0^\theta, R_0^\theta$ respectively represents the parameter initial value of parameter observer EKFθ, the initial value of covariance matrix of parameter estimation error, the initial value of system process noise, and the initial value of observation noise; x_0, P_0^x, Q_0^x, R_0^x respectively represents the initial value of the CKFx state of the state observer, the initial value of the covariance matrix of the state estimation error, the initial value of the system process noise, and the initial value of the observation noise;

Step 1: Priori estimation of parameters-$\hat{\theta}_k^-$

$$\theta_k^- = \theta_{k-1}, P_k^{\theta,-} = P_{k-1}^\theta + Q_{k-1}^\theta \quad (3)$$

Step 2: Priori estimation of state-$\hat{x}_{k|k-1}^{-}$

$$x_{k|k-1} = f(x_{k-1}, \bar{\theta}_k, u_{k-1},), x^{-}_{k|k-1} = \quad (4)$$

$$\frac{1}{m}\sum_{i=1}^{m} x_{k|k-1} + q^{x}_{k-1}$$

$$P^{x}_{k|k-1} = (1/m)\sum_{i=1}^{m} x_{k|k-1} x^{T}_{k|k-1} - \bar{x}_{k|k-1} x^{T,-}_{k|k-1} + Q^{x}_{k-1} \quad (5)$$

Step 3: Posteriori estimation of state-$\hat{x}_{k|k-1}$

Innovation matrix:

$$e^{x}_{k} = y_k - \left(\frac{1}{m}\sum_{i=1}^{m} h(x_{k|k-1}, \bar{\theta}_k, u_k) + \hat{r}^{x}_{k-1}\right) \quad (6)$$

Gain matrix:

$$K^{x}_{k} = \left((1/m)\sum_{i=1}^{m} x_{k|k-1} y^{T}_{k|k-1} - x_{k|k-1} y^{T}_{k|k-1}\right) \times \quad (7)$$

$$\left((1/m)\sum_{i=1}^{m} y_{k|k-1} y^{T}_{k|k-1} - y_{k|k-1} y^{T}_{k|k-1} + R^{x}_{k}\right)^{-1}$$

System status correction:

$$x_k = \bar{x}_{k|k-1} + K^{x}_{k} e^{x}_{k} \quad (8)$$

Error covariance correction:

$$P^{x}_{k} = P^{x}_{k|k-1} - \quad (9)$$

$$K^{x}_{k}\left((1/m)\sum_{i=1}^{m} y_{k|k-1} y^{T}_{k|k-1} - y_{k|k-1} y^{T}_{k|k-1} + R^{x}_{k}\right) K^{x,T}_{k}$$

Step 4: Posteriori estimation of parameters -$\hat{\theta}_k$

Innovation matrix:

$$e^{\theta}_{k} = y_k - \left(\frac{1}{m}\sum_{i=1}^{m} h(x_{k|k-1}, \bar{\theta}_k, u_k)\right) \quad (10)$$

Gain matrix:

$$K^{\theta}_{k} = P^{\theta,-}_{k}\left(C^{\theta}_{k}\right)^{T}\left(C^{\theta}_{k} P^{\theta,-}_{k}\left(C^{\theta}_{k}\right)^{T} + R^{\theta}_{k-1}\right)^{-1} \quad (11)$$

System parameter correction:

$$\theta_k = \bar{\theta}_k + K^{\theta}_{k} e^{\theta}_{k} \quad (12)$$

Covariance update of system parameter estimation error:

$$P^{\theta}_{k} = \left(I - K^{\theta}_{k} C^{\theta}_{k}\right) P^{\theta,-}_{k} \quad (13)$$

$$C^{\theta}_{k} = \frac{dg(x_k, \theta_k, u_k)}{d\theta} = \frac{\partial g(x_k, \theta_k, u_k)}{\partial \theta} + \quad (14)$$

$$\frac{\partial g(x_k, \theta_k, u_k)}{\partial x}\frac{dx_k}{d\theta}$$

$$\frac{dx_k}{d\theta} = \frac{\partial f(x_{k-1}, u_k, \theta)}{\partial \theta} + \frac{\partial f(x_{k-1}, u_k, \theta)}{\partial x_{k-1}}\frac{dx_{k-1}}{d\theta}$$

In addition, in the process of calculating C_k^{θ}, it is necessary to solve the partial derivative of the state quantity concerning the number of parameters. In the case that the a priori estimated value of $dx_k/d\theta$ is unknown, the initial value of $dx_k/d\theta$ is set to zero.

Improvement of cubature Kalman filter

Introduce in random weighting factor

Traditional CKF filtering requires accurate priori statistical characteristics of measurement noise. When the statistical characteristics of measurement noise are unknown, the filtering accuracy will significantly decrease or even diverge.

However, in the actual operation process, complex operating conditions and a changeable operating environment will cause changes in the statistical characteristics of noise. Some scholars use the moving window method to adaptively update the statistical characteristics of system noise and iterate the error covariance matrix to ensure the numerical stability of the algorithm, which improves the filtering accuracy of the algorithm to a certain extent. However, they all ignore the differences in the contribution of information at different times, so they can't accurately estimate the statistical characteristics of measurement noise, which has a certain impact on the filtering accuracy. In this chapter, the random weighting factor is introduced to estimate the statistical characteristics of the system noise, and the adaptive adjustment of the weight of the cubature point is realized, so as to improve the estimation accuracy of the system and further restrain the interference of the statistical characteristics of noise to the system [20-22].

Random weighting factors are defined as follows:

$$\begin{cases} \Delta x_j = \hat{x}_k - \bar{x}_{k|k-1}, \Delta y_j = \hat{y}_k - y_{k|k-1} \\ \left\|\Delta x_j\right\| = \sqrt{\Delta x_j^T \Delta x_j} \left\|\Delta y_j\right\| = \sqrt{\Delta y_j^T \Delta y_j} \\ \lambda_j = \left\|\Delta x_j\right\| \left\|\Delta y_j\right\| \Big/ \sum_{j=1}^{2n} \left\|\Delta x_j\right\| \left\|\Delta y_j\right\| \quad (j = 1, 2, \ldots, 2n) \end{cases} \tag{15}$$

In which, Δx_j as the state residual vector; Δy_j as the observation residual vector; λ_j as the random weighting factor.

The noise adaptive update process is as follows, and its derivation process has been described in detail in reference [23], there is no repeat it here:

System process noise and covariance matrix

$$\begin{cases} q_k^x = \frac{1}{k}\left[(k-1)q_{k-1}^x + \bar{x}_{k|k-1} - \sum_{i=1}^{2n} \lambda_i x_{k|k-1}\right] \\ Q_k^x = \frac{1}{k}\left[\begin{array}{l}(k-1)Q_{k-1}^x + K_k^x K_k^{x,T} + P_{k|k-1}^x - \\ \sum_{i=1}^{m} \lambda_i \left(x_{k|k-1} x_{k|k-1}^T\right) - \bar{x}_{k|k-1} x_{k|k-1}^T\end{array}\right] \end{cases} \tag{16}$$

Systematic observation noise and covariance matrix

$$\begin{cases} \hat{r}_k^x = \frac{1}{k}\left[(k-1)\hat{r}_{k-1}^x + y_{k|k-1} - \sum_{i=1}^{2n} \lambda_i y_{k|k-1}\right] \\ R_k^x = \frac{1}{k}\left[(k-1)R_{k-1}^x - (\sum_{i=1}^{m} \lambda_i y_{k|k-1} y_{k|k-1}^T - y_{k|k-1} y_{k|k-1}^T)\right] \end{cases} \tag{17}$$

Introduce in singular value decomposition

When CKF deal with the problem of non-linear system state filtering, the state error covariance matrix needs to keep symmetry and positive definiteness all the time. However, in practical application, the covariance matrix loses positive definiteness due to computer truncation error, unknown statistical characteristics of system noise, and abnormal model disturbance, which leads to system instability and even stagnation. Therefore, this chapter introduces Singular Value Decomposition (SVD) to improve the stability of the algorithm [20,24].

$$\begin{aligned} P_{k-1}^x &= U_{k-1} S_{k-1} V_{k-1}^T \\ x_{k-1|k-1} &= U_{k-1} \sqrt{S_{k-1}} \zeta_i + x_{k-1}, i = 1, \ldots, 2n \end{aligned} \tag{18}$$

SOC estimation of lithium-ion power battery based on EKF-ARWCKF filtering

Establishment of system model

System modeling is an important means and foundation to study a practical system. For the same system, different research methods and purposes will lead to differences in models. As the most widely used battery model, the equivalent circuit model can't accurately explain the changes in external characteristics caused by the internal variables of the battery, but its model is simple, the amount of calculation is small, and the accuracy of the model can meet the needs of practical engineering, so it is widely used in real vehicle BMS [25,26]. In reference [27], the n-RC equivalent circuit model is established by distinguishing the number of RC nodes, and the equivalent circuit models of different orders are evaluated uniformly based on the AIC principle. The results show that the 1-order RC model has the best balance between model complexity and computation. In addition, the research of this dissertation focuses more on the establishment and verification of the parameter and state co-estimation algorithm, so this dissertation intends to use the 1-order RC model as the model basis in the follow-up research, which is shown in Fig. 2.

Based on Kirchhoff's electric current law and the characteristics of electrical components, the following discrete systems are established:

$$\begin{cases} U_{D,k} = \exp\left(\frac{-\Delta t}{C_D R_D}\right) U_{D,k-1} + \\ \qquad \left(1 - \exp\left(\frac{-\Delta t}{C_D R_D}\right)\right) i_{L,k-1} R_D \\ U_{t,k} = U_{OC,k} - U_{D,k} - i_{L,k} R_0 \end{cases} \tag{19}$$

It is known that the Kalman filtering process can be divided into two parts: prediction and correction, that is to say after the prior prediction is completed by the system state equation, the prior prediction value is modified based on the feedback link of terminal voltage error and the optimal state a posteriori estimation is obtained. Therefore, this chapter takes the SOC estimation of power battery as an example to explain the prior estimation and posterior estimation process in detail.

(1) Priori estimation of SOC

A priori estimation is the preliminary prediction of the state quantity, which requires relatively low accuracy,

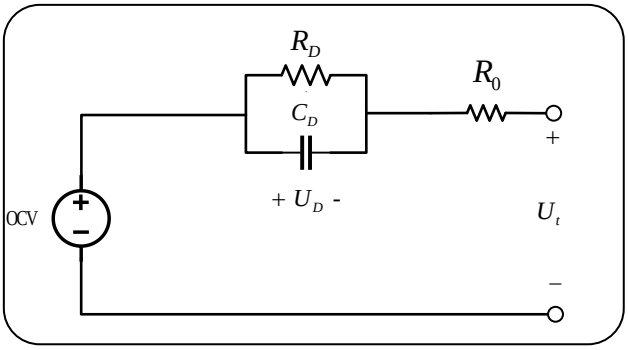

Fig 2: Schematic Diagram of 1order RC Battery Model.

but it should reflect the increase and decrease of SOC in the process of battery charge-discharge in real-time. The Ampere-hour method is often used for a priori estimation of SOC because of its small amount of computation and high real-time performance, as shown in Eq.(20).

$$z_{k+1} = z_k - \frac{\eta_k i_{L,k} \Delta t}{C_a} \tag{20}$$

Where, z_k represent the SOC estimate of k-moment; Δt is the data sampling interval; η_k represent the coulombic efficiency of the battery, which is related to the battery charge-discharge rate, operating conditions, and other factors. In view of the fact that the tests in this dissertation are carried out under laboratory conditions, the default value is 1.

(2) SOC posterior estimation

A posteriori estimation corrects the prior estimation of the state through the feedback link, which directly determines the estimation accuracy and optimization efficiency of SOC. The mapping relationship between the open-circuit voltage and SOC is relatively little affected by environment temperature, operating conditions, and other factors, and always maintains a monotonous mapping relationship, so the OCV-SOC fitting relationship is usually chosen as the feedback link of a priori estimation. Establish the OCV-SOC mapping relationship as follows:

$$U_{oc,k} = a_0 + a_1 z_k + a_2 z_k^2 + a_3 z_k^3 + \tag{21}$$

$$a_4 / z_k + a_5 \ln(z_k) + a_6 \ln(1 - z_k)$$

In the flow of modeling, it is assumed that the maximum available capacity of the battery is accurately known (the co-estimation of SOC and capacity will be discussed in the following chapters). Parameter quantities include ohmic internal resistance $R_{0,k}$, polarization internal resistance $R_{D,k}$ and polarization capacitance $C_{D,k}$, and the state quantities include polarization voltage $U_{D,k}$ and charged state z_k. The model parameters obtained by the online identification strategy and the input battery terminal voltage and electric current can be used to estimate the state of the power battery in real-time. In this dissertation, a co-estimation algorithm based on state and parameters is used to estimate the SOC accurately.

The state matrix and parameter matrix are defined as follows:

$$x_k = [U_{D,k}, z_k]^T \tag{22}$$

$$\theta_k = [R_{0,k}, R_{D,k}, C_{D,k}]^T \tag{23}$$

By reconstructing the equation (19) according to the above definition, the state equation and observation equation based on extended Kalman filter- EKF-ARWCKF filtering co-estimation can be obtained:

$$\begin{cases} x_{k+1} = f(x_k, \theta_k, u_k) \\ \quad = \begin{bmatrix} \exp\left(\frac{-\Delta t}{C_{D,k} R_{D,k}}\right) & 0 \\ 0 & 1 \end{bmatrix} x_k + \\ \quad \begin{bmatrix} \left[1 - \exp\left(\frac{-\Delta t}{C_{D,k} R_{D,k}}\right)\right] i_{L,k} R_{D,k} \\ \eta_k i_{L,k} \Delta t / C_a \end{bmatrix} \\ y_{k+1} = g(x_{k+1}, \theta_{k+1}, u_{k+1}) = U_{oc,k} - U_{D,k} - i_{L,k} R_{0,k} \end{cases} \tag{24}$$

Where,y_k represent terminal voltage and u_k as the terminal electric current. The above mathematical relationship is the mathematical model of SOC estimation algorithm based on EKF-ARWCKF filtering.

SOC co-estimation algorithm based on 1-order RC Model

The flow and the model construction for the co-estimation algorithm of parameters and state have been described in detail in section 1.1, in a nutshell, the current state of the battery is accurately estimated based on the obtained parameters and then the accurate state estimation is used to estimate the parameters of the model at the next time. However, considering the slow time-varying characteristics of the model parameters and the fast time-varying characteristics of the system state, it is difficult to co-estimate them

on a unified time scale. So the problem of time scale will be studied in the following chapters. This chapter only considers the co-estimation problem under a single-time scale.

The correlation matrix in the system state equation and measurement equation is defined as follows:

$$A_{k-1}=\begin{bmatrix}\exp\left(\frac{-\Delta t}{C_{D,k}R_{D,k}}\right) & 0\\ 0 & 1\end{bmatrix} \tag{25}$$

$$C_k^x=\begin{bmatrix}-1 & \frac{\partial U_{oc}(\hat{z}_k^-)}{\partial z_k^-}\end{bmatrix} \tag{26}$$

$$C_k^\theta=\begin{bmatrix}-1 & 0 & 0\end{bmatrix}^T+C_k^x\frac{\partial x_k}{\partial \theta_k^-} \tag{27}$$

Available from formula

$$\frac{\partial U_{oc}}{\partial z}=a_1+2a_2z+3a_3z^2- \tag{28}$$

$$a_4/z^2+a_5/z+a_6/(1-z)$$

And

$$\frac{dx_k}{d\theta}=\frac{\partial f(x_{k-1},\theta,u_{k-1})}{\partial\theta}+A_{k-1}\frac{dx_{k-1}}{d\theta} \tag{29}$$

$$\frac{\partial f\left(x_{k-1},\theta,u_{k-1}\right)}{\partial\theta}=\begin{bmatrix}0 & c_1 & c_2\\ 0 & 0 & 0\end{bmatrix} \tag{30}$$

$$\begin{cases}c_1=\frac{U_{D,k-1}\Delta t}{R_{D,k}^2C_{D,k}}\exp\left(\frac{-\Delta t}{C_{D,k}R_{D,k}}\right)-\\ \quad\frac{i_{L,k-1}\Delta t}{C_{D,k}R_{D,k}}\exp\left(\frac{-\Delta t}{C_{D,k}R_{D,k}}\right)-\\ \quad i_{L,k}\left[\exp\left(\frac{-\Delta t}{C_{D,k}R_{D,k}}\right)-1\right]\\ c_2=\frac{U_{D,k-1}\Delta t}{R_{D,k}^2C_{D,k}}\exp\left(\frac{-\Delta t}{C_{D,k}R_{D,k}}\right)-\\ \quad\frac{i_{L,k-1}\Delta t}{C_{D,k}^2}\left(\frac{-\Delta t}{C_{D,k}R_{D,k}}\right)\end{cases} \tag{31}$$

During the operation of the BMS system, the current and voltage signals measured and loaded by the sensor in real time are transferred into the EKF-ARWCKF filter to co-estimate the state and parameters of the power battery. Fig. 3 is a flow chart of the algorithm based on EKF-ARWCKF filtering.

Calculation case and experimental verification

Lithium-ion power battery bench

In this dissertation, the ternary lithium-ion battery with a rated capacity of 2Ah is taken as the test object, and the basic characteristics of the ternary lithium-ion battery are tested through the lithium-ion power battery test bench to obtain the required test data. The lithium-ion power battery test bench is mainly composed of a power battery tester (Neware BTS), a thermostat (DF-GDW) used to change the test environment temperature, and an upper computer used to control the test process and store test data, as shown in Fig. 4.

The Neware BTS (Battery Test System) has 16 test channels, the voltage test range of each channel is 0-5 V, and the measurement inaccuracy is less than 0.05%. It can test the characteristics of the power battery according to the preset charge-discharge strategy in the upper computer and collect the current, voltage, charge-discharge capacity, and other information in real-time, and upload the relevant information to the upper computer for storage. The thermostat can adjust the environment temperature in the range of -40 ℃-80 ℃, then realize the characteristic test under different temperature conditions, and analyze the characteristics of the power battery at different temperatures. The upper computer is used to formulate the charge-discharge strategy, control the test process and store the test data. The information on the power battery and the test equipment used in this dissertation are shown in the following Table 1.

Verification and Analysis of EKF-CKF Series filtering algorithms

In order to further improve the filtering effect, the random weighting theory and singular value decomposition are introduced into the cubature Kalman filtering process to adaptively adjust the cubature point weight and system noise while improving the stability of the algorithm. In this section, during the verification process, the initial value of SOC is set to 60% (the precise value is 80%), and the filtering results of FRLS-EKF, EKF-CKF, and EKF-ARWCKF algorithms under DST operating conditions (25 ℃) are compared, as shown

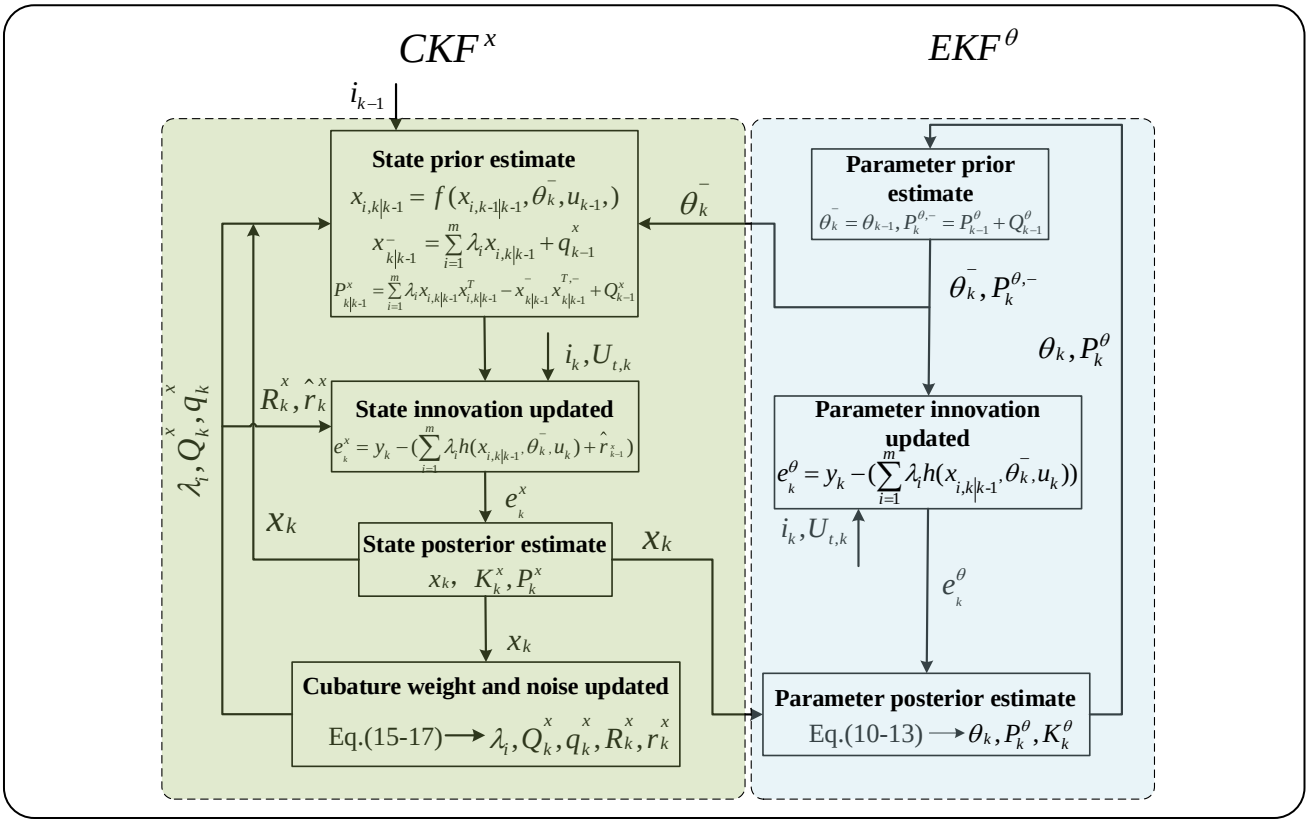

Fig 3: Flow Chart Based on EKF-ARWCKF Filtering Algorithm.

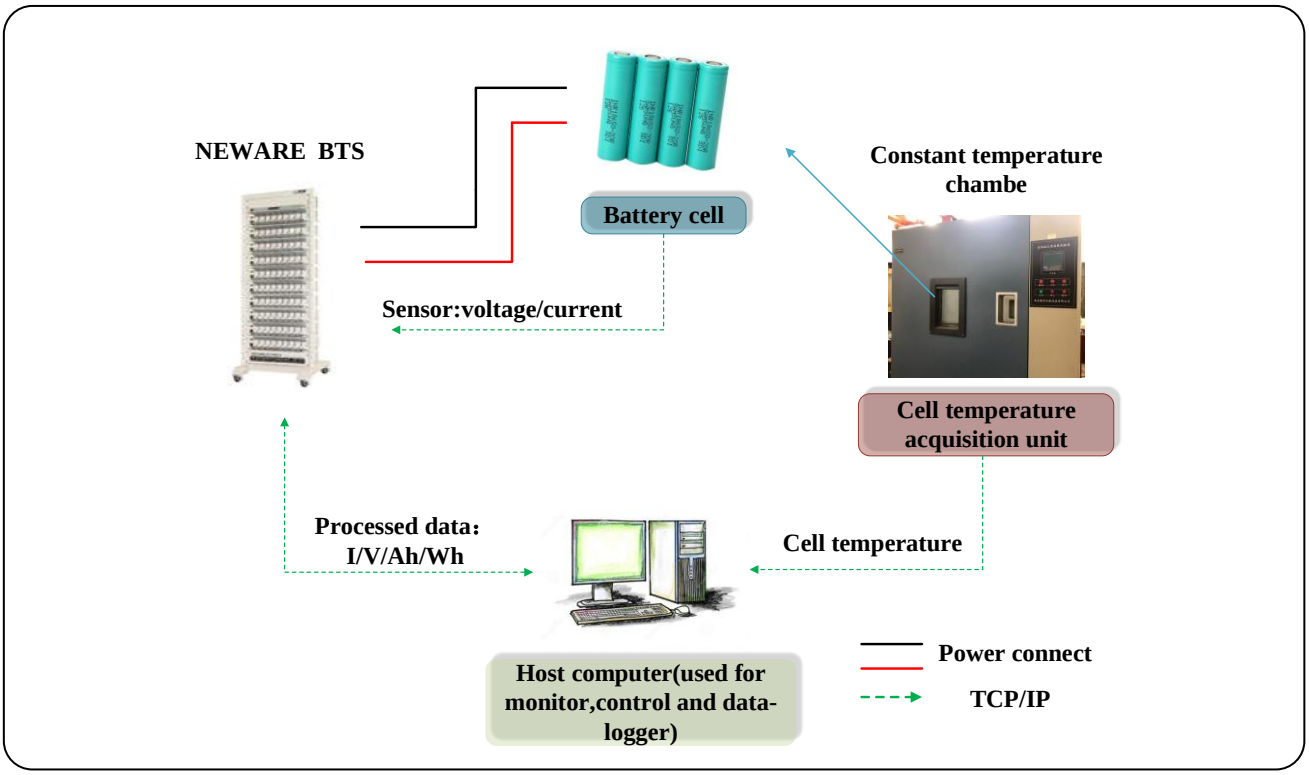

Fig 4: Configuration of Battery Test Bench.

Table 1: Main parameters of the battery cell.

Battery type	Nominal voltage	Charging cut-off voltage	Discharging cut-off voltage	Rated capacity
LNMC/Graphite	3.6 V	4.2 V	2.9 V	2 Ah

Table 2: Main Parameters of the battery test system.

Performance index	Parameter
Number of channels	16
Single-channel voltage range	0-5 V
Single-channel current range	0-10 A
Current / Voltage control accuracy	0.05%
Data acquisition interval	1 Hz/10 Hz/50 Hz/100 Hz
Communication	TCP/IP

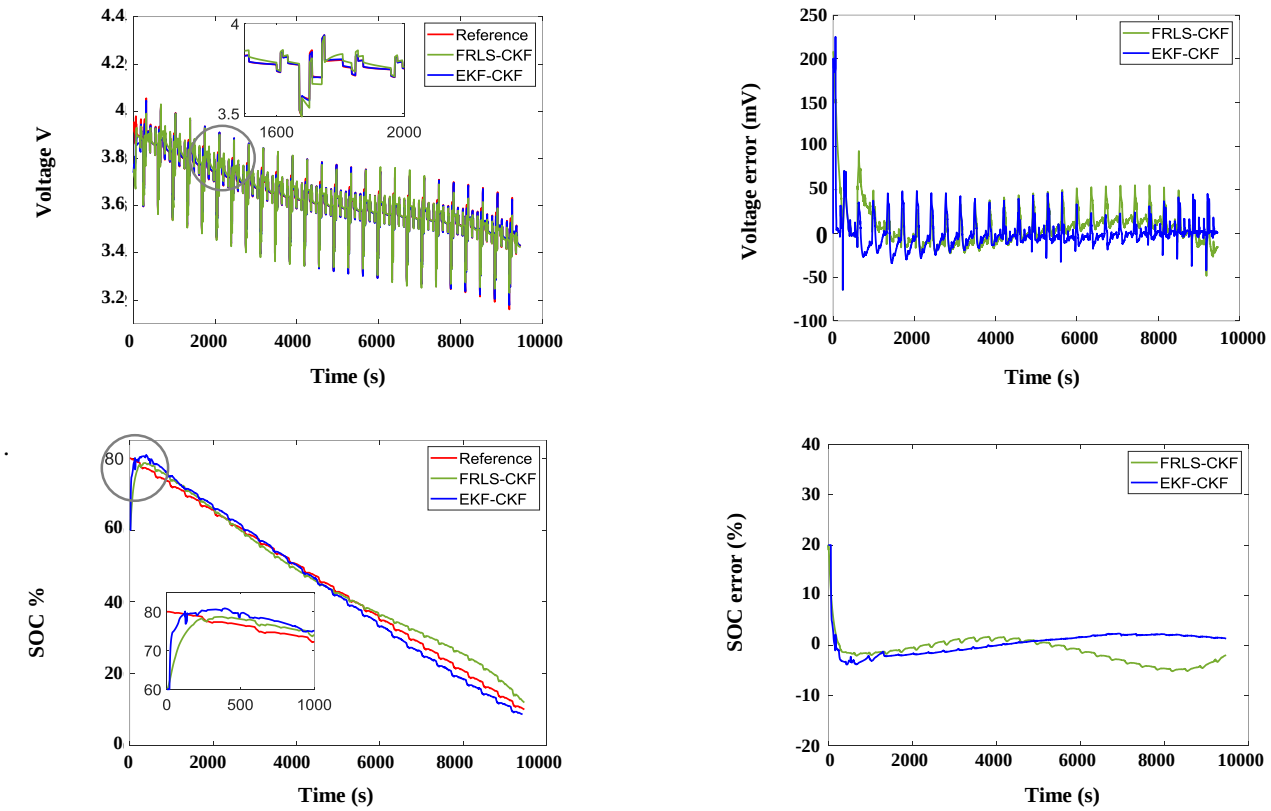

Fig 5: Comparative Analysis of Filtering Results Between FRLS—CKF and EKF—CKF.

in Fig. 5 and Fig. 6. From the comparison results, it is found that the co-estimation algorithm of parameter and state based on EKF-CKF filter can not only improve the prediction accuracy of terminal voltage and SOC, but also converge to the reference value faster when the initial value of SOC is inaccurate, which has better robustness.

The filtering results of the above three algorithms are simply summarized as shown in Table 3, which can be seen from the above error analysis results: (1) the extended Kalman filter is used to replace the least square method based on genetic factors for online identification of model parameters, the co-estimation of model parameters and

Table 3: Main Parameters of Battery Test System

Filtering method	SOC root mean square error (%)	SOC maximum absolute error (%)	Terminal voltage root mean square error (mV)	Maximum absolute error of terminal voltage (mV)	SOC convergence time(s)
EKF—CKF	1.39	2.90	13.88	80.00	80
EKF—ARWCKF	1.40	3.00	14.06	78.00	78

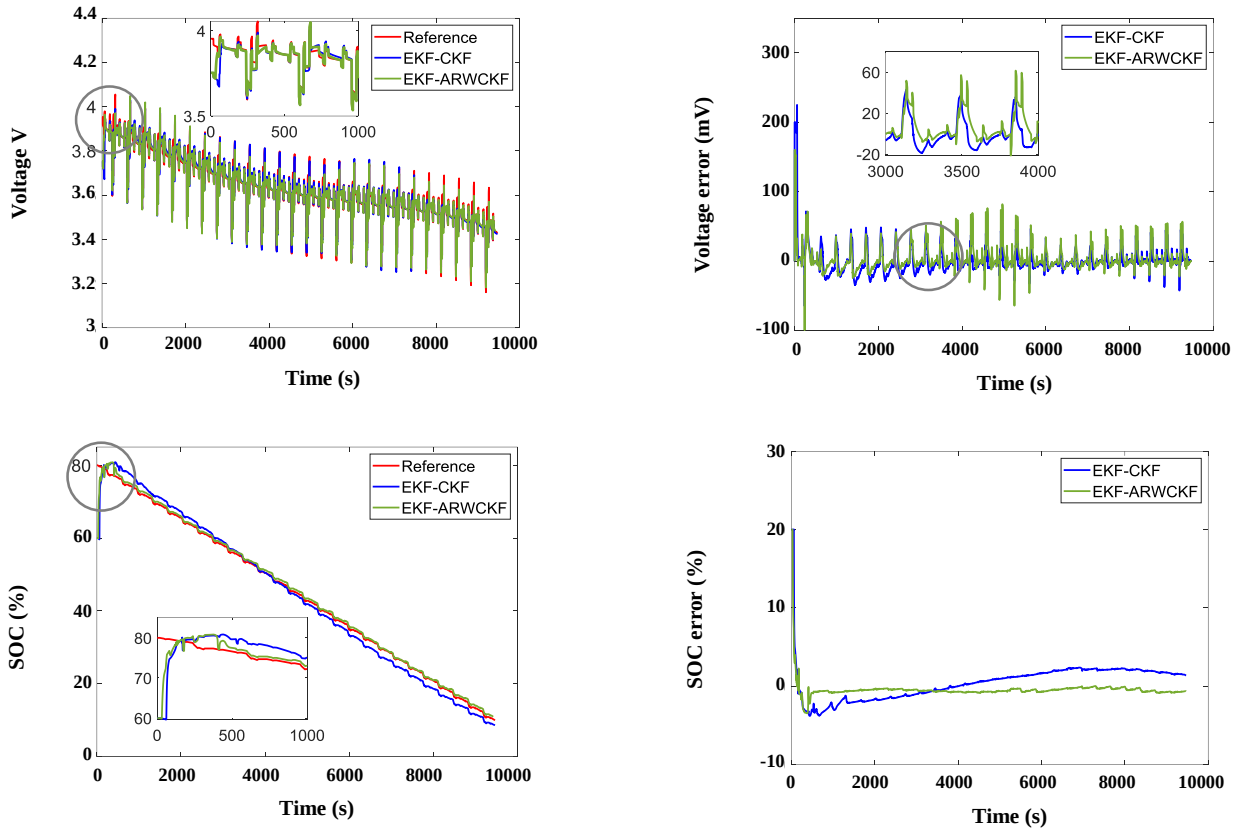

Fig 6: Comparative Analysis of Filtering Results Between EKF—CKF and EKF—ARWCKF (a)Prediction result of terminal voltage; (b)Terminal voltage prediction error; (c)SOC prediction result; (d) SOC prediction error.

the state is realized, then the posterior estimation of the state is used to correct the priori estimation of parameters, which further improves the accuracy of parameter identification and state prediction. Based on the DST operating condition data at 25 ℃, the results show that the co-estimation of parameter and state algorithm based on EKF-CKF filter can not only improve the prediction accuracy of terminal voltage and SOC, but also converge to the reference value faster when the initial value of SOC is inaccurate and has better robustness. (2) Random weighting factor and noise adaptive process are introduced in the EKF-CKF filtering process to update the system noise while adaptively adjusting the weight of the cubature point, which suppresses the influence of the fixed weight of the cubature point and noise sensitivity on the CKF filtering process, is more suitable for practical applications. The DST operating condition data at 25 ℃are also used for comparative verification, and the results show that the introduction of the random weighting factor does not significantly improve the filtering effect. In view of the singleness of the experimental data selected in this section, the effect and significance of the improved al will be further verified.

RESULTS AND DISCUSSION

Time scale is the average measurement of the time for a system to complete a process. In the actual battery system, the time-varying characteristics of the parameters and the state are obviously different. Usually, the state of

the system has the characteristic of fast time-varying, and the system parameter has the characteristic of slow time-varying. If the system parameters and states are estimated by taking the data sampling interval as the unified time scale, the stability of the algorithm will be decreased and the computational load of the algorithm will be increased if the system parameters change too frequently. Finally, it has an impact on the stability and response speed of the estimation algorithm. Furthermore, some scholars co-estimate the system parameters and state based on two kinds of time scales, that is to say, the system states are estimated by the micro time scale, and the system parameters are modified under the macro time scale. The two-time scales are relatively fixed and the macro scale is a fixed multiple of the microscale [27]. Compared with the single time scale, the dual time scale avoids the operational load caused by the fluctuation of system parameters and improves the stability of the algorithm to a certain extent, but it also has some limitations. First of all, there is a lack of reasonable theoretical support for the macro-scale for the correction of system parameters, and the algorithm is highly volatile at different macro-scales. In addition, the fixed time scale of system parameter estimation is difficult to be widely applied to complex and changeable real vehicle operating conditions, and the estimation of system parameters will be significantly affected when the change of SOC is small or the charge-discharge current is small in a fixed time interval. In addition, some scholars have proposed to use a certain amount of SOC change as the conversion standard between micro and macro time scales, that is to say, to set the SOC change threshold to complete the time update of the model parameters. Although it avoids the disadvantages caused by the fixed-parameter update scale to a certain extent, the SOC estimation error also brings uncertainty to the capacity estimation [28]. In practical application, the measurement accuracy of current is obviously higher than the estimation of SOC[29], so this section takes the influence of temperature as an example to realize the co-estimation of SOC at different temperatures based on EKF-ARWCKF filtering algorithm. In view of the different time-varying characteristics between battery state and parameters, further-more, the co-estimation algorithm of parameters and state under variable-time-scale is proposed and compared with the estimation results under single-time-scale.

Establishment of non-linear discrete system under variable-time-scale

$$\begin{cases} x_{k+1} = f(x_k, \theta_i, u_k) + w_k \\ \theta_{l+1} = \theta_l + \rho_l \\ y_{k+1} = g(x_{k+1}, \theta_{i+1}, u_{k+1}) + v_{k+1} \end{cases} \tag{32}$$

Where, k represents the sampling point of the system at the moment of t_k, the time scale of state estimation is consistent with the data sampling interval; l represents the time scale of system parameter estimation. In this dissertation, the cumulative discharge capacity is used as the conversion standard between micro-scale and macro-scale, that is to say, the system parameters are estimated at regular intervals of cumulative capacity discharge (Ll is the scale conversion limit value); $\theta_l$represents the system parameter vector identified on-line by the algorithm at the sampling time of $t_{\sum L_l}$, which will be used as the model parameter value of the state estimation in the next L_{l+1} sampling interval and the meaning of the other parameters is consistent with that of the Eq.(24). Here, the parameter matrices $P_k^\theta, Q_k^\theta, R_k^\theta$ in a single-time-scale in section 1.1 are rewritten into $P_l^\theta, Q_l^\theta, R_l^\theta$ in variable-time-scale. the principle of the filtering algorithm is shown in Fig. 7.

Co-estimation of SOC and capacity under variable-time-scale

Based on the 1-order RC equivalent circuit model establishes the non-linear discrete system of power battery as shown in Eq.(33). The feedback and correction of the prior estimates of the state and model parameters of the variable time scale EKF-ARWCKF system are also based on the terminal voltage error, and then the accurate a posteriori estimates are obtained.

$$\begin{cases} U_{D,k} = \exp\left(\dfrac{-\Delta t}{C_{D,l} R_{D,l}}\right) U_{D,k-1} + \\ \qquad \left(1 - \exp\left(\dfrac{-\Delta t}{C_{D,l} R_{D,l}}\right)\right) i_{L,k-1} R_{D,l} \\ U_{t,k} = U_{OC,k} - U_{D,k} - i_{L,k} R_{0,l} \end{cases} \tag{33}$$

The feedback link of the co-estimation of capacity and SOC will be built here.

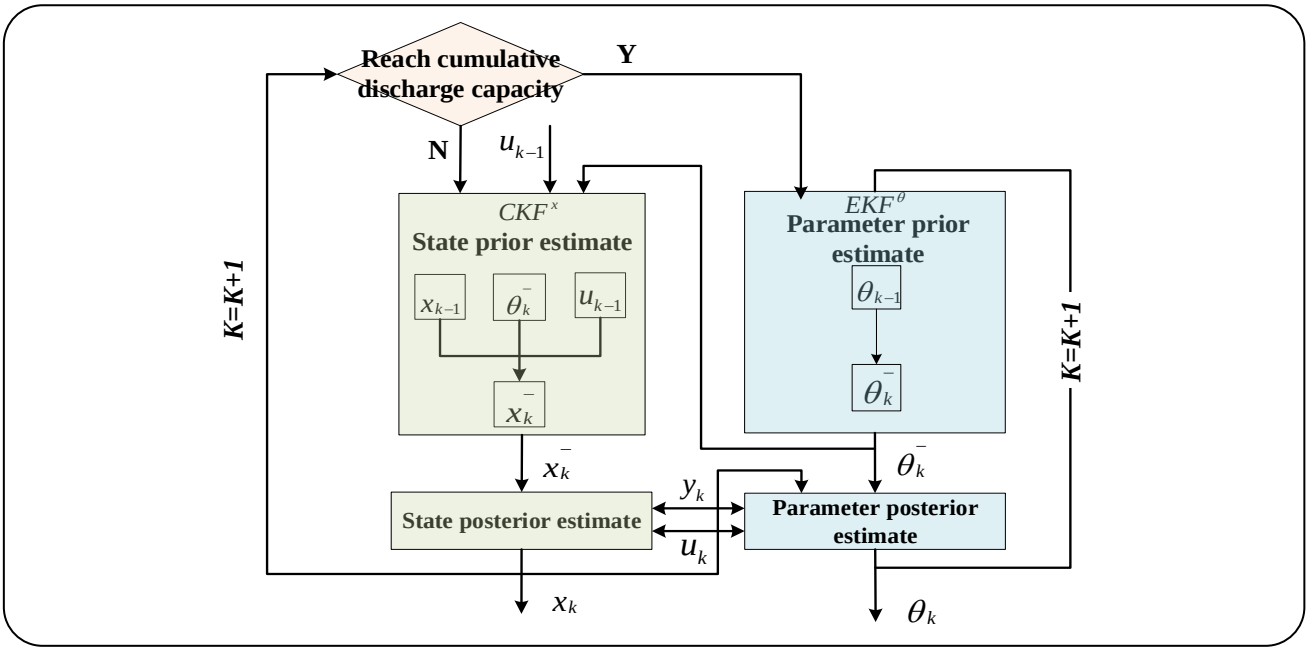

Fig 7: Variable Time Scale Filtering Based on EKF-ARWCKF Algorithm.

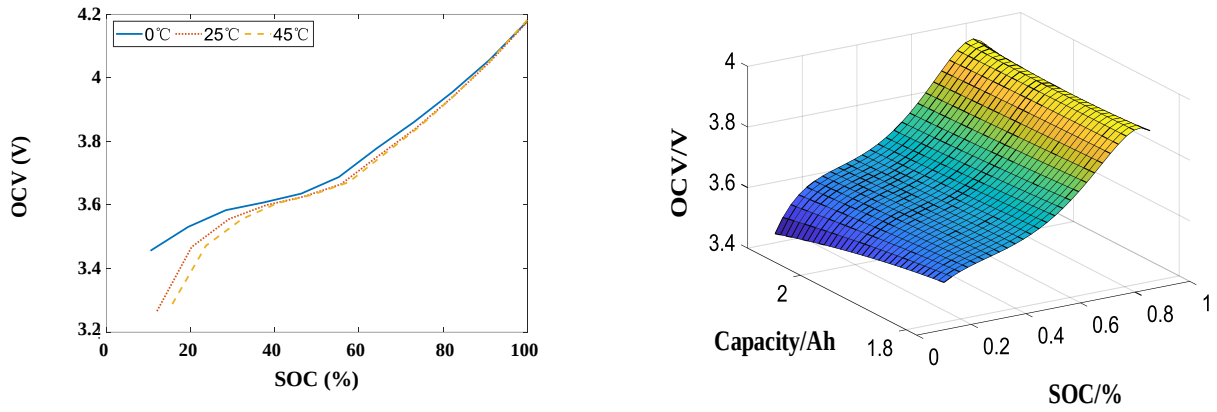

Fig 8: Capacity—SOC—OCV Three-Dimensional Response Surface.

For the same type of battery, the OCV-SOC relationship is relatively stable, so it is often chosen as the feedback link of SOC[30,31]. However, in the process of practical application, the battery aging degree and using temperature will affect it, and the most intuitive reflection of the aging degree, using temperature and other factors of the battery is the capacity, that is to say, when effectively estimate the battery capacity, we should fully consider the changes of battery aging degree, considering temperature and OCV-SOC relationship[32,33]. Therefore, this section is based on the OCV-SOC relationship under different capacities, whose mapping relationship is shown in Eq.(34). The capacity—SOC-OCV three-dimensional response surface shown in Fig. 8 is established to provide accurate feedback on capacity and SOC.

$$U_{oc,k}\left(C_{a,l}, z_k\right) = a_0 + a_1 z_k + a_2 z_k^2 + a_3 z_k^3 + a_4 / z_k + a_5 \ln\left(z_k\right) + a_6 \ln\left(1 - z_k\right) \quad (34)$$

It should be noted here that the polynomial coefficients b_0 to b_6 are no longer constants, which are quadratic functions related to capacity:

$$\left[b_0\ b_1\ b_2\ b_3\ b_4\ b_5\ b_6\right]^T = \Lambda \times \left[C_{a,l}^2\ C_{a,l}\ 1\right] \quad (35)$$

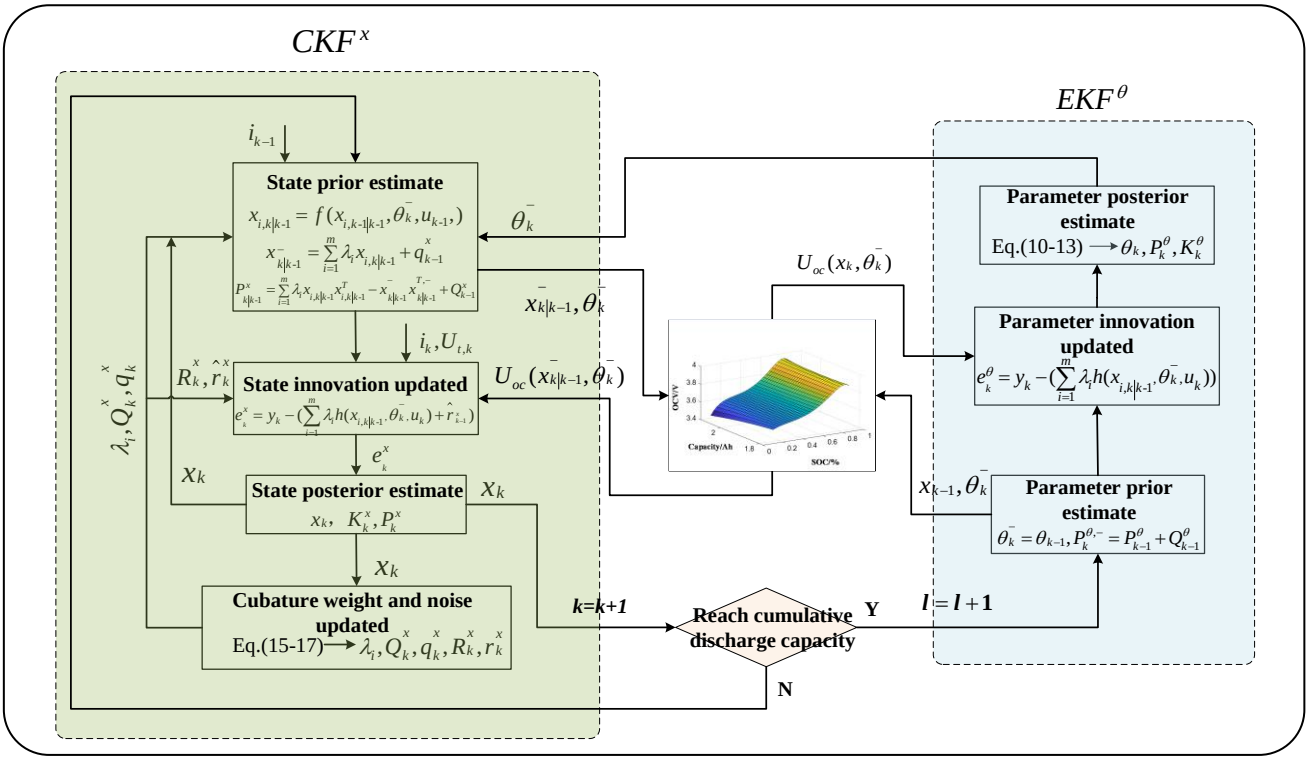

Fig 9: Flow Chart Based on Variable Time Scale EKF-ARWCKF Filtering Algorithm.

In which, Λ is 7 × 3, which is obtained by fitting the OCV-SOC relationship with different capacities, and $C_{a,l}$ represent the capacity value obtained by feedback correction at $t_{\sum L_l}$ monent.

Based on the above model relationship, the system state and parameter matrix are defined respectively as shown in the Eqs.(36-37). The state matrix includes polarization voltage $U_{D,k}$ and charge state z_k, which is updated once at each sampling interval, and the parameter matrix includes ohmic internal resistance $R_{0,l}$, polarization internal resistance $R_{D,l}$, polarization capacitance $C_{D,l}$ and battery capacity $C_{a,l}$, which is modified every L_l sampling interval.

$$x_k = \begin{bmatrix} U_{D,k} & z_k \end{bmatrix} \tag{36}$$

$$\theta_l = \begin{bmatrix} R_{0,l} & R_{D,l} & C_{D,l} & C_{a,l} \end{bmatrix} \tag{37}$$

The state equation and observation equation suitable for EKF-ARWCKF filtering can be obtained by reorganizing the definition of charge state, system discrete equation, state, and parameter matrix.

$$\begin{cases} x_{k+1} = f(x_k, \theta_l, u_k) = \begin{bmatrix} \exp\left(\dfrac{-\Delta t}{C_{D,l} R_{D,l}}\right) & 0 \\ 0 & 1 \end{bmatrix} x_k + \\ \qquad \begin{bmatrix} [1 - \exp\left(\dfrac{-\Delta t}{C_{D,l} R_{D,l}}\right)] i_{L,k} R_{D,l} \\ \eta_k i_{L,k} \Delta t / C_{a,l} \end{bmatrix} \\ y_{k+1} = g(x_{k+1}, \theta_{l+1}, u_{k+1}) = U_{oc,k} - U_{D,k} - i_{L,k} R_{0,l} \end{cases} \tag{38}$$

There established the discrete mathematical model of the variable-time-scale EKF-ARWCKF filtering algorithm in this chapter. Based on this, the subsequent chapters will study the co-estimation of capacity and SOC. The overall flow of the co-estimation filtering algorithm is shown in Fig. 9.

Calculation case and experimental verification

In this section, during the verification process, the filtering algorithm is debugged with the basic characteristic test data at three fixed environment temperatures (0 ℃, 25 ℃, 45 ℃). Based on the experimental data of FUDS at room temperature, the algorithm is verified and analyzed under the condition that the initial values

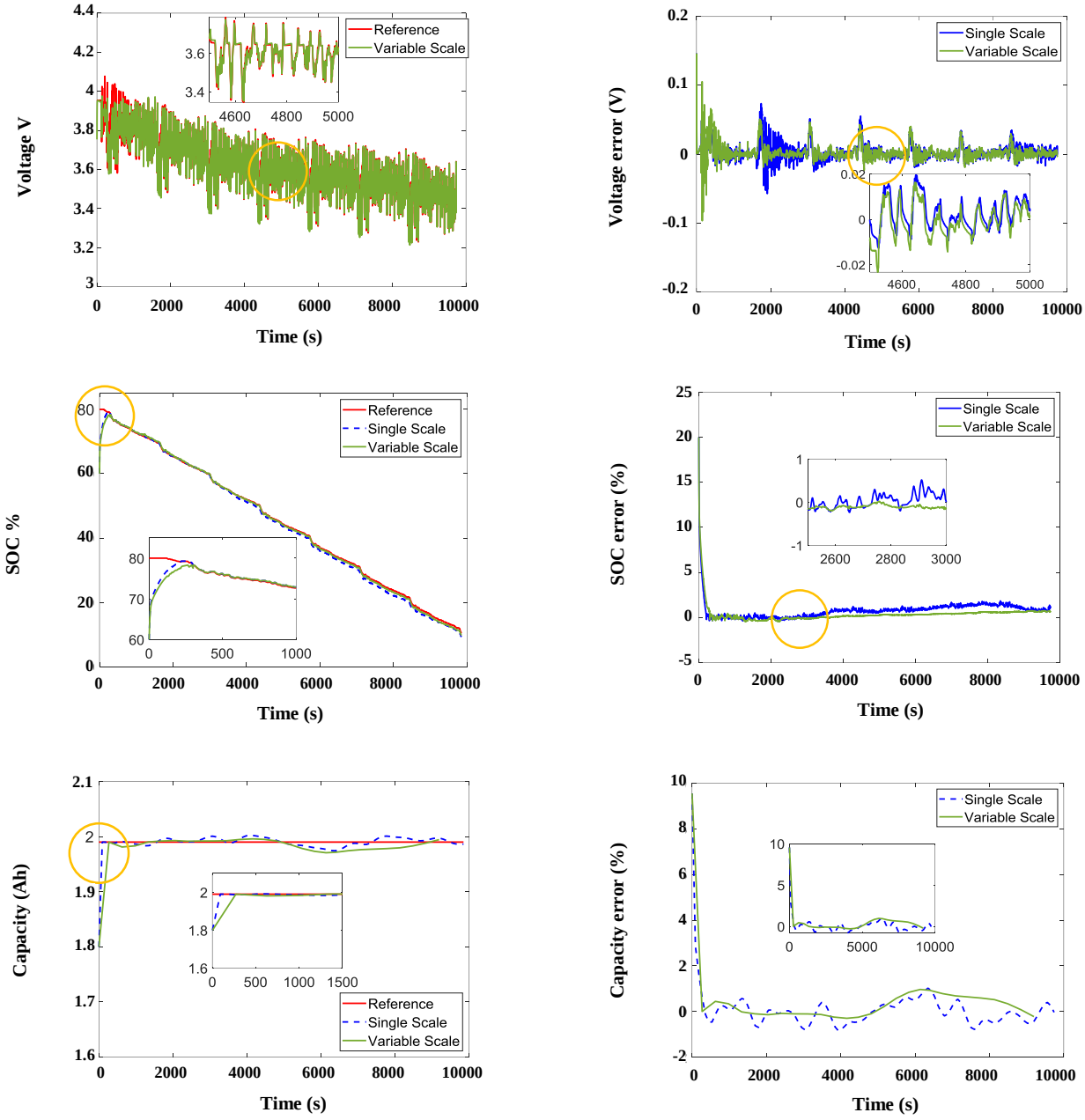

Fig 10: Comparative Analysis of Variable Time Scale EKF-ARWCKF Filtering Algorithm: (a) terminal voltage filtering results comparison (b) terminal voltage prediction error; (c) SOC filtering results comparison; (d) SOC estimation error; (e) capacity filtering results comparison; (f) capacity prediction error ratio.

of SOC and capacity are not accurate. In addition, this section sets the scale conversion limit value L (that is to say, discharge capacity) to 0.06 Ah. Finally, the prediction results of single-time-scale and variable-time-scale algorithms are compared, and the advantages and disadvantages of the algorithm are analyzed in detail.

Based on the detailed analysis of the filtering results of variable-time-scale, the following conclusions can be obtained: (1) after the algorithm converges to stability, the absolute error of terminal voltage is basically below 70.00 mV, as shown in Fig.10(a) and (b); (2) according to the prediction results and errors of SOC (Fig. 10(c) and (d), the algorithm can converge to less than 5.00% error within 107 seconds, and the SOC estimation error after converging to stability is less than 1.00%; (3) Fig (e) and (f) show that the predicted capacity can converge to the reference value

Table 4: Comparison of EKF-ARWCKF filtering results between single-time-scale and multiple-time scale.

Filtering algorithm	Terminal voltage root mean square error (mV)	SOC root mean square error (%)	Capacity root mean square error (%)
Single-time-scale EKF—ARWCKF	11.27	1.17	4.93
Variable-time scale EKF—ARWCKF	9.82	0.94	3.17

for the first time within 271 s, and the capacity error after convergence is less than 2.00%. It should be noted that the 271 s is the macro-time-scale of the first capacity update, which is related to the setting of the scale conversion standard and does not represent the exact time of the algorithm convergence. Therefore, it is of little significance to compare with the capacity convergence rate under a single-time scale.

Through the above comparison, it can be found that the EKF-ARWCKF filtering results under the variable-time scale are better than the single-time- scale in most error indexes. The advantages of the co-estimation algorithm of system state and parameters are as follows: By constantly modifying the model parameters and system state quantities, the terminal voltage error is gradually reduced to the minimum, so that the state prediction result is based on terminal voltage error feedback is to optimality. However, considering the slow time-varying characteristics of the parameter quantity of the system and the fast time-varying characteristics of state quantity, if a single-time-scale is used, the algorithm will frequently modify system parameters unnecessarily to improve the prediction accuracy of terminal voltage, thus weakening the feedback of terminal voltage to state prediction and even affecting the accuracy of state estimation. At the same time, imprecise state estimators will affect the correction of system parameters, and ultimately reduce the accuracy and stability of the filtering algorithm. Table 4 shows the error characteristics of the two algorithms, which more directly reflects the advantages and disadvantages of the two algorithms, and verifies the rationality of the above results.

CONCLUSIONS

In the process of practical application, the maximum available capacity of the battery is not a definite value. As many factors will affect it, it is difficult to obtain its accurate value. Based on the research of co-estimation of state and parameters, this dissertation introduces the maximum available capacity of the battery into the system parameter matrix, and finally completes the co-estimation of capacity and SOC. The comparison between EKF-ARWCKF and EKF-CKF under a single time scale shows that, the improved method has a similar accuracy with EKF-CKF and a better convergence speed.In view of the different time-varying characteristics between the system parameters and state, the cumulative discharge is selected as the time-scale conversion standard, and the co-estimation algorithm of capacity and SOC under variable-time-scale is constructed. Based on the basic characteristic test and cycling condition test data, the EKF--ARWCKF filtering algorithm in single-time-scale and variable-time-scale is verified under the condition of inaccurate SOC and initial capacity. The filtering results of two algorithms are compared and analyzed from the aspects of: terminal voltage prediction accuracy, SOC estimation accuracy, and capacity estimation accuracy. The results in Table.4 show that the accuracy of the variable-time-scale algorithm is better than that of the single-time-scale algorithm, and the amount of computation is significantly reduced.

In future research, it will not only be limited to the single battery, but also consider the co-estimation of power batteries in different groups, and make an in-depth study on the capacity recession model of power batteries.

Acknowledgments

This research is funded by the Natural Science Basic Research Program of Shaanxi (Grant no. 2020-JQ-913), Supported by "the Fundamental Research Funds for the Central Universities, CHD (Grant no. 300102220503), College-Level Research Fund of Xi'an Aeronautical Institute (Grant no. 2020KY0219).

Received : Oct. 25, 2021 ; Accepted : Dec. 4, 2021

REFERENCES

[1] Ma J., Liu X.D, Chen Y.S., The present situation and Countermeasures of the Development of New Energy vehicle Industry and Technology in China. *China J. Highway Transport*, **31(08)**: 1-19 (2018).

[2] "The State Council released the Development Plan of Energy Saving and New Energy Automobile Industry" (2012-2020).

[3] Chemali E., Kollmeyer P.J., Preindl M., Emadi A., State-of-charge Estimation of Li-Ion Batteries Using Deep Neural Networks: A Machine Learning Approach, *J. Power Sources*, **400**: 242-255 (2018).

[4] Manane Y., Yazami R., Accurate State of Charge Assessment of Lithium-Manganese Dioxide Primary Batteries, *J. of Power Sources*, **359**: 422-426 (2017).

[5] Ramadan H.S., Becherif M., Claude F., 2017. Extended Kalman Filter for Accurate State of Charge Estimation of Lithium-Based Batteries: A Comparative Analysis. *Int. J. Hydrog. Energy*, **42(48)**: 29033-29046 (2017).

[6] Chen X., Shen W., Cao Z., Kapoor A., 2014. A novel Approach for State of Charge Estimation Based on Adaptive Switching Gain Sliding Mode Observer in Electric Vehicles, *J. Power Sources*, **246**: 667-678 (2014).

[7] Gallardo-Lozano J., Romero-Cadaval E., Milanes-Montero M.I., Guerrero-Martinez M.A., Battery Equalization Active Methods, *J. Power Sources*, **246**: 934-949 (2014).

[8] Khan M.R., Mulder G., Van Mierlo J., An Online Framework for State of Charge Determination of Battery Systems Using Combined System Identification Approach, *J. Power Sources*, **246**: 629-641 (2014).

[9] Moura S.J., Chaturvedi N.A., Krstić M., Adaptive Partial Differential Equation Observer for Battery State-of-Charge/State-of-Health Estimation *via* an Electrochemical Model, *J. Dyn. Syst., Measur., Cont.*, **136(1)**: (2014).

[10] Plett G.L., Extended Kalman Filtering for Battery Management Systems of LiPB-based HEV Battery Packs: Part 3. State and Parameter Estimation, *J. Power sources*, **134(2)**: 277-292 (2004).

[11] Lee S., Kim J., Lee J., Cho B.H., State-of-Charge and Capacity Estimation of Lithium-Ion Battery Using a New Open-Circuit Voltage Versus State-of-Charge. *J. Power Sources*, **185(2)**: 1367-1373 (2008).

[12] Yue Z., Lian B., Tang C., "The Gps/Ins Integrated Navigation Method Based on Adaptive Ssr-Sckf Cubature Kalman Filter", *China Satell. Navigat. Conf.*, 395-405 (2017).

[13] Arasaratnam I., Haykin S., Cubature Kalman Filters, *IEEE Trans. Auto. Cont.*, **54(6)**: 1254-1269 (2009).

[14] Zhang H., Xie J., Ge J., Lu W., Liu B., Strong Tracking SCKF Based on Adaptive CS Model for Manoeuvring Aircraft Tracking, *IET Radar, Sonar Navig.*, **12(7)**: 742-749 (2018).

[15] Hu Y., Zhang S., Luo L. Fault Diagnosis of Gas Circuit Components of Turbofan Engine Based on Adaptive Volume Kalman Filter, *Journal of Aerospace Power*, **31(5)**: 1260-1267 (2016).

[16] Xinglong T.A.N., Jian W.A.N.G., Changsheng Z.H.A.O., Neural Network Aided Adaptive UKF Algorithm for GPS/INS Integration Navigation, *Acta Geod. Cartogr. Sin.*, **44**(4): 384 (2015).

[17] Gao W.G., He H.B., Chen J.P., 2008. An Adaptive UKF Algorithm and its Application for GPS/INS integrated Navigation System, *Trans. Beijing Ins. Technol.*, **28**: 505-509 (2008).

[18] Mahmood A., Wang, J.L., Machine Learning for High Performance Organic Solar Cells: Current Scenario and Future Prospects, *Energ. Environ. Sci.*, **14(1)**: 90-105 (2021).

[19] Lin J., Second Order Tail Approximation for the Maxima of Randomly Weighted Sums with Applications to Ruin Theory and Numerical Examples, *Stat. Probabil. Lett.*, **153**: 37-47 (2019).

[20] Gao S., Zhong Y., Shirinzadeh B., Random Weighting Estimation for Fusion of Multi-Dimensional Position Data, *Inf. Sci.*, **180(24)**: 4999-5007 (2010).

[21] Gao Z., Mu D., Zhong Y., Gu C., Ren C., Adaptively Random Weighted Cubature Kalman Filter for Nonlinear Systems, *Math. Probl. Eng.*, **2019**: (2019)

[22] Xu X., Luo M., Tan Z., Pei R., Echo Signal Extraction Method of Laser Radar Based on Improved Singular Value Decomposition and Wavelet Threshold Denoising, *Infrared Phys. Technol.*, **92**: 327-335 (2018).

[23] Cho S., Jeong H., Han C., Jin S., Lim J.H., Oh J., State-of-Charge Estimation for Lithium-Ion Batteries under Various Operating Conditions Using an Equivalent Circuit Model, *Comput. Chem. Eng.*, **41**: 1-9 (2012).

[24] Duan Y., "Study on SOC Estimation Method of Lithium-Ion Battery for Electric vehicle". Ph.D. Thesis, Hunan University, Changsha, China (2018).

[25] Xiong R., "Research on State Estimation of Electric Vehicle Power Battery Pack Based on Data Model Fusion". PhD, Thesis, Beijing Institute of Technology, Beijing, China (2014).

[26] Jiang B., Dai H., Wei X., Xu T., Joint Estimation of Lithium-Ion Battery State of Charge and Capacity within an Adaptive Variable Multi-Timescale Framework Considering Current Measurement Offset, *Appl. Energy*, **253**: 113619 (2019).

[27] Xiong R., Yu Q., Lin C., A Novel Method to Obtain the Open Circuit Voltage for the State of Charge of Lithium Ion Batteries in Electric Vehicles by Using H Infinity Filter, *Appl. Energy*, **207**: 346-353 (2017).

[28] Tian Y., Lai R., Li X., Xiang L., Tian J., A Combined Method for State-of-Charge Estimation for Lithium-Ion Batteries Using a Long Short-Term Memory Network and an Adaptive Cubature Kalman Filter, *Appl. Energy*, **265**: 114789 (2020).

[29] Dong G., Wei J., Chen Z., Sun H., Yu X., Remaining Dischargeable Time Prediction for Lithium-Ion Batteries Using Unscented Kalman Filter, *J. Power Sources*, **364**: 316-327 (2017).

[30] Kenney B., Darcovich K., MacNeil D.D., Davidson I.J., Modelling the Impact of Variations in Electrode Manufacturing on Lithium-Ion Battery Modules, *J. Power Sources*, **213**: 391-401 (2012).

[31] Zhang C., Allafi W., Dinh Q., Ascencio P., Marco J., Online Estimation of Battery Equivalent Circuit Model Parameters and State of Charge Using Decoupled Least Squares Technique, *Energy*, **142**: 678-688 (2018).